Ponderomotive generation of density cavities from kinetic Alfvén wave–slow-mode coupling in Earth's high-β plasma sheet

Mani K Chettri[1], Hemam D. Singh[2], Rupak Mukherjee[1]

[1] *Department of Physics, Sikkim University, Gangtok 737102, Sikkim, India*

[2] *Department of Physics, Netaji Subhas University of Technology, New Delhi 110078, India*

Introduction

Localized depletions in plasma density and magnetic field, known as density cavities and magnetic holes, are commonly observed in Earth's magnetotail plasma sheet, and their origin remains debated [1, 2, 3]. One candidate is the pressure of kinetic Alfvén waves (KAWs), shear Alfvén waves whose perpendicular wavelength is comparable to the ion-sound gyroradius ρ_s or the ion gyroradius ρ_i; at these scales the wave becomes dispersive and acquires a parallel electric field [5, 6]. Carrying a field-aligned Poynting flux, KAWs are a major channel for kinetic-scale energy transport in the collisionless plasma sheet [7, 8], where the plasma beta is often of order unity or larger [9, 10, 11] and the response to the wave pressure is strong. That a KAW can carve a density cavity through its own pressure is well established: its magnetic pressure acts as a ponderomotive force that expels plasma from high-amplitude regions [12, 13, 14], supporting KAW envelope solitons and Zakharov-type density structuring [15, 16, 17]. These reduced-model studies establish the mechanism but do not follow a localized packet over many wave periods, nor test the predicted response against multiple in-situ intervals. Here we extend previous studies in three ways: (i) a time-dependent two-field calculation showing that a localized packet develops into a long-lived, co-located cavity rather than dispersing or collapsing; (ii) recovery of the quasi-static density law, and its breakdown near $\beta \approx 1$, in a system where no density law is imposed; and (iii) a region-matched, multi-interval MMS test of the density–magnetic anti-correlation.

Reduced two-fluid model

In a uniform background of density n_0 and field $\mathbf{B}_0 = B_0\hat{\mathbf{z}}$, in the low-frequency, strongly anisotropic ordering $\omega \ll \Omega_i$, $k_\perp \gg k_\parallel$, the transverse KAW field δB_y propagates refractively through the slow density n it creates, while n responds acoustically to the gradient of the KAW ponderomotive potential $U_{\rm pond} = |\delta B_y|^2/16\pi$ [12, 18]. Normalizing length by $L_\perp$ ($\perp$) and $L_\parallel$ ($\parallel$), time by $L_\parallel/v_A$, the field by B_0 and density by n_0, with $b = \delta B_y/B_0$ and $\eta = n/n_0$, gives

$$\partial_{tt} b - \partial_{zz}\big(1 - \alpha\,\partial_{xx}\big) b + \partial_z(\eta\,\partial_z b) = 0, \qquad \partial_{tt}\eta - \mu\big(\lambda^2\partial_{xx} + \partial_{zz}\big)\eta = \tfrac{1}{4}\big(\lambda^2\partial_{xx} + \partial_{zz}\big)(b^2), \quad (1)$$

with v_A the Alfvén speed, $\alpha = (\rho_s/L_\perp)^2$, $\mu = (c_s/v_A)^2 = \beta/2$, $\lambda = L_\parallel/L_\perp$, and $\beta = 8\pi n_0(T_e + T_i)/B_0^2$ the total-pressure plasma beta. The first equation recovers the KAW dispersion $\omega^2 = k_\parallel^2 v_A^2(1 + k_\perp^2\rho_s^2)$; the $\frac{1}{4}(b^2)$ term is the ponderomotive drive. In the high-β plasma sheet the slow mode is strongly ion-Landau damped, so the density responds quasi-statically: setting $\partial_{tt}\eta \to 0$ slaves η to the wave intensity, and we adopt the published quasi-static KAW ponderomotive density law [15, 16]

$$\eta = -\frac{1}{2(1+\beta)}\,|b|^2, \tag{2}$$

in our total-temperature β convention. It reduces to the static limit $\eta \to -|b|^2/(2\beta)$ of Eq. (1) at high β; at the fiducial $\beta = 2$ the ponderomotive slope is $\eta/|b|^2 = -1/[2(1+\beta)] = -0.167$. Equations (1) and the closure are solved with a 2-D Fourier pseudospectral method on a periodic (x,z) domain with $2/3$ dealiasing, advancing each mode's linear part with an exact propagator and the nonlinear forcing by a Strang (kick–drift–kick) splitting. The fiducial run uses a 128^2 grid on a $100 \times 100\,\rho_s$ box, $\Delta t = 0.02$, $t = 0$–500 (≈ 80 ion-cyclotron periods), $\beta = 2$, $\alpha = 1$. The scheme is second order in Δt (measured order 2.09), reproduces the linear KAW dispersion to relative error $\leq 3 \times 10^{-4}$, and is grid-converged at 256^2 (slope identical, depth within 1%).

Results

A localized packet evolves into a coherent magnetic enhancement accompanied by a co-located density depletion, an ion-scale ($\approx 20\,\rho_s$) magnetic-hole-like cavity that neither disperses nor collapses (Fig. 1). The simulated density falls on the ponderomotive line $\eta = -|b|^2/[2(1+\beta)]$ with a fitted slope -0.167 ($R^2 = 1.00$), the density minimum coinciding with the magnetic maximum; an amplitude scan confirms the $\propto A^2$ depth scaling (fitted exponent 2.0), and the depletion reaches $|\delta n/n_0| \approx 4.5 \times 10^{-4}$ on average (up to $\approx 1.5 \times 10^{-3}$ at the center) for $|b| \approx 0.03$–0.09. Since the closure is imposed here, this slope is a consistency check; the stricter test is the time-dependent two-field model, in which η is advanced by its own weakly damped wave equation rather than tied to $|b|^2$. At $\beta = 2$, with the same grid, domain, and initial condition, a localized depletion forms, stays co-located with the wave-intensity maximum, and persists for the full integration ($\gtrsim 80$ ion-cyclotron periods) at a depth (late-time mean $\approx 1.4 \times 10^{-3}$) comparable to the quasi-static run; the cavity and its persistence are therefore not artefacts of the imposed density law. A β-scan of this system, with no density law imposed, recovers the high-β slope $-1/(2\beta)$ to within $\approx 15\%$ for $\beta \geq 2$ (ratio 1.12, 1.07, 0.99 at $\beta = 2, 4, 8$) and converges to it at large β, while at $\beta \approx 1$ the closure breaks down, bracketing its regime of validity. A quasi-static-closure verification run at $\beta = 0.76$ (the total β of the 2017-05-31 crossing below) forms the same long-lived cavity with the correspondingly stronger coefficient

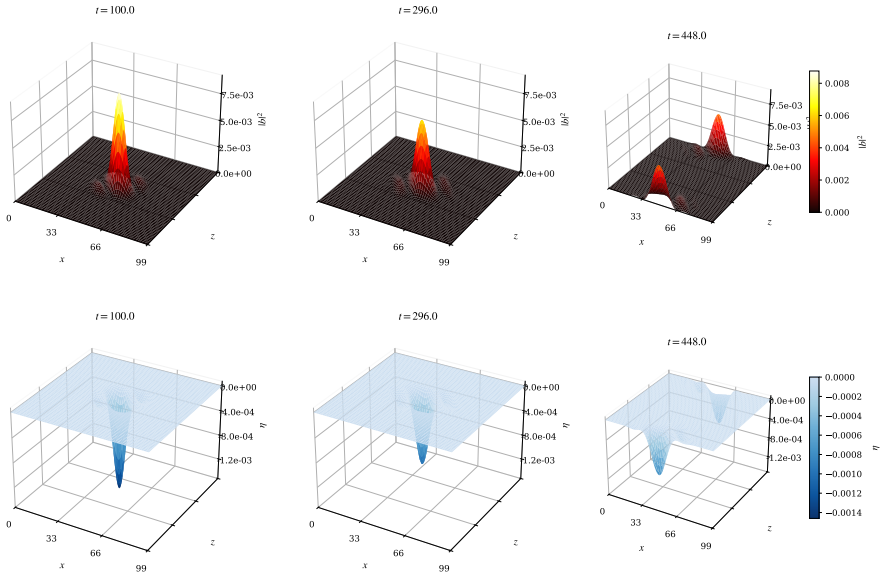

Figure 1: Field evolution of a self-focusing KAW packet at $t = 100, 296, 448$: the magnetic intensity $|b|^2$ (top) grows into a coherent enhancement while the density η (bottom) develops a co-located, ion-scale cavity.

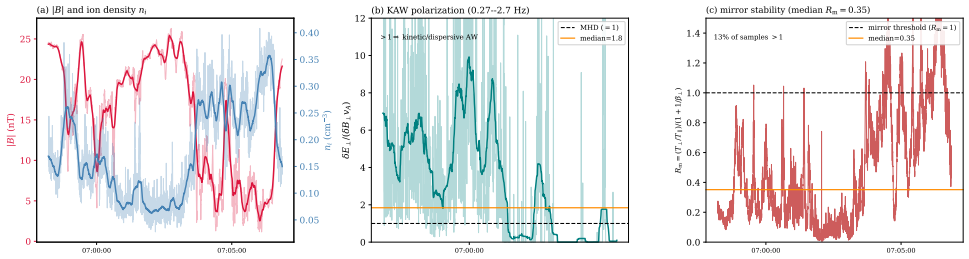

Figure 2: MMS-1 plasma-sheet KAW interval (2017-07-26). (a) $|B|$ and ion density n_i. (b) Polarization $\delta E_\perp/(\delta B_\perp v_A) \approx 1.8$. (c) Mirror discriminator R_m (median 0.35): mirror-stable.

$-1/[2(1+\beta)] = -0.284$.

Comparison with observations

The model couples density to the KAW magnetic *intensity* $|\delta B_\perp|^2$; in spacecraft data this reads as an anti-correlation between density and the *total* field $|B|$, since a compressive KAW and quasi-static pressure balance $\delta(B^2/2\mu_0) \approx -\delta p$ place the depletion at the magnetic-pressure maximum. Model and data are compared through the *sign* of the correlation, the KAW identification, and mirror stability, not a slope, since this linear anti-correlation is equally the signature of compressional pressure balance (the direct quadratic relation lies below the turbulent noise here).

A separate check distinguishes the ponderomotive interpretation from a mirror-mode origin: the mirror instability requires $R_\mathrm{m} = (T_\perp/T_\parallel)/(1+1/\beta_\perp) > 1$ [4], yet 52 of the 56 plasma-sheet holes of Sun et al. [1] lie below this threshold. We analyze an MMS-1 burst-mode KAW interval in the magnetotail plasma sheet (2017-07-26, 06:58:13–07:06:52 UT; Fig. 2), using FGM [20], FPI ion moments [21], and EDP electric-field data [22, 23] from the MMS mission [19, 24]. In

the order-unity-β plasma sheet ($\beta_i \approx 1.0$, $\beta_{\rm tot} \approx 1.7$, near the fiducial regime) it shows a density–magnetic anti-correlation of the predicted sign (Pearson $r = -0.18$, 95% CI $[-0.24, -0.12]$, Spearman $\rho = -0.25$; $N = 3460$ ion samples). Its polarization $\delta E_\perp/(\delta B_\perp v_A) \approx 1.8$ and finite compressibility $|\delta B_\parallel|/|\delta B_\perp| \approx 0.45$ at ion scales ($\rho_i \approx 420$ km) identify a kinetic Alfvén wave. A field-aligned ion-temperature analysis places it in the mirror-stable region (median $R_{\rm m} \approx 0.35$), so its anti-correlation is not a mirror signature but is consistent with the KAW ponderomotive response. The anti-correlation is not specific to one window: the same analysis procedure applied to a separate, previously reported PSBL KAW crossing on 2017-05-31 [25] yields the same negative sign in every burst segment, significant where β is appreciable ($r = -0.25$ to -0.10) and null only in the tenuous lobe-like approach ($\beta_i \approx 0.16$), all mirror-stable. The predicted anti-correlation therefore recurs across two independent magnetotail crossings ($\beta_i \approx 0.4$–1.0). In physical units the modeled cavity maps to ~ 8500 km (≈ 1.3 Earth radii) with a $\approx$ 5-min lifetime for the measured parameters ($|B| \approx 17.4$ nT, $n_i \approx 0.16$ cm^{-3}).

Conclusions

Ponderomotive KAW–slow-mode coupling forms long-lived, ion-scale ($\approx 20\rho_s$) density cavities in high-β plasma, with depth following the quasi-static law $\eta = -|b|^2/[2(1+\beta)]$ ($\propto A^2$, weakening with β); the same persistent, co-located cavity emerges in the time-dependent two-field system for $\beta \geq 2$, with closure breakdown near $\beta \approx 1$. Region-matched, mirror-stable MMS intervals from two independent magnetotail crossings show the predicted density–magnetic anti-correlation, supporting (though, being shared with compressional pressure balance, not uniquely proving) ponderomotive coupling as a plausible origin for hole-like cavities in the high-β magnetotail.

References

[1] W. J. Sun *et al.*, *Annales Geophysicae* **30**, 583 (2012).

[2] X.-J. Zhang *et al.*, *Journal of Geophysical Research: Space Physics* **122**, 6174 (2017).

[3] S. Y. Huang *et al.*, *The Astrophysical Journal* **875**, 113 (2019).

[4] S. P. Gary, *Journal of Plasma Physics* **35**, 431 (1986).

[5] A. Hasegawa and L. Chen, *Physics of Fluids* **19**, 1924 (1976).

[6] R. L. Lysak and W. Lotko, *Journal of Geophysical Research* **101**, 5085 (1996).

[7] J. R. Wygant *et al.*, *Journal of Geophysical Research* **107**, 1201 (2002).

[8] J. E. Stawarz *et al.*, *Geophysical Research Letters* **44**, 7106 (2017).

[9] W. Baumjohann, G. Paschmann, and C. A. Cattell, *Journal of Geophysical Research* **94**, 6597 (1989).

[10] W. Baumjohann *et al.*, *Journal of Geophysical Research* **93**, 11507 (1988).

[11] T. E. Eastman *et al.*, *Journal of Geophysical Research* **89**, 1553 (1984).

[12] V. I. Karpman, *Journal of Plasma Physics* **27**, 215 (1982).

[13] S. R. Spangler, *Physics of Fluids B* **1**, 1738 (1989).

[14] P. Bellan and K. Stasiewicz, *Physical Review Letters* **80**, 3523 (1998).

[15] A. B. Mikhailovskii, V. I. Petviashvili, and A. M. Fridman, *JETP Letters* **24**, 43 (1976).

[16] K. Stasiewicz *et al.*, *Space Science Reviews* **92**, 423 (2000).

[17] R. P. Sharma and H. D. Singh, *Journal of Geophysical Research* **114**, A03109 (2009).

[18] V. E. Zakharov, *Soviet Physics JETP* **35**, 908 (1972).

[19] J. L. Burch, T. E. Moore, R. B. Torbert, and B. L. Giles, *Space Science Reviews* **199**, 5 (2016).

[20] C. T. Russell *et al.*, *Space Science Reviews* **199**, 189 (2016).

[21] C. Pollock *et al.*, *Space Science Reviews* **199**, 331 (2016).

[22] R. E. Ergun *et al.*, *Space Science Reviews* **199**, 167 (2016).

[23] P.-A. Lindqvist *et al.*, *Space Science Reviews* **199**, 137 (2016).

[24] V. Angelopoulos *et al.*, *Space Science Reviews* **215**, 9 (2019).

[25] Z. Zhang *et al.*, *Earth and Planetary Physics* **6**, 465 (2022).